28

Novel Methods for Diagnosis of Pulmonary Microangiopathy in Diabetes Mellitus

Kalicka Renata and Kuziemski Krzysztof
Gdansk University of Technology, Department of Biomedical Engineering,
Medical University of Gdansk, Department of Allergology,
Poland

1. Introduction

Lung microangiopathy is a little known negative influence of diabetes mellitus on the functioning of the lungs. In current medical practice lung microangiopathy is diagnosed by comparing two measurements of lung diffusing capacity – one with the subject standing and one with the subject lying. The necessity to take two measurements is inconvenient.

In lung microangiopathy we observe a reduction of diffusing capacity, lung flow and volume. Diabetes is a chronic illness that can lead to diabetic angiopathy, a pathology of the blood vessels (arteries, veins and capillaries). There are two types of diabetic angiopathy: macroangiopathy (disease of the larger blood vessels) and microangiopathy (microvascular pathology). The examples of angiopathy include: neuropathy, nephropathy and retinopathy.

Current knowledge regarding diabetic lung microangiopathy is limited. Histopathological examination of lung biopsy samples is not a conclusive test of the consequences of diabetes (Dalquen, 1999). Animal experiments and post-mortem examinations have disclosed the influence of diabetes on the lung capillaries and alveolar-capillary membranes (Kida et al, 1993), (Kodolova et al, 1982) and (Popov& Simionescu, 1997). Histopathological tests have revealed the thickening of the alveolar and venous capillary walls (Matsubara& Hara, 1991) and (Weynand et al, 1999).

Lung diffusing capacity measurements illustrate the state of alveolar-capillary barrier (Goldman, 2003). These are measurements of diffusion across the alveolar-capillary membrane. For diagnosing microangiopathy, the lung diffusing capacity is measured in two body positions: standing (D_L^{standing}) and lying on the back (D_L^{lying}), (Strojek et al, 1993) and (Kuziemski et al, 2008). On account of the human anatomic structure, diffusing capacity depends on the body's position. For healthy subjects the diffusing capacity increases in the reclined position, $D_L^{\text{lying}} > D_L^{\text{standing}}$. The opposite is observed in the case of microangiopathic patients: the diffusing capacity decreases when the subject is lying $D_L^{\text{lying}} < D_L^{\text{standing}}$. This is the result of blood vessel damage and alveolar thickening caused by diabetes (Kuziemski et al, 2009). Only the fact that diffusing capacity increases or decreases in a given position is important as far as microangiopathy diagnosis is concerned.

Spirometry (measurement of the volume and flow of inhaled and exhaled air) is the most common pulmonary function test. It is helpful in diagnosing asthma, pulmonary fibrosis, cystic fibrosis, and COPD (Chronic Obstructive Pulmonary Disease).

Research (Goldman, 2003), (Kaminski, 2004) has shown that a single spirometry test does not provide sufficient information for a diagnosis of lung flow limitation and lung volume reduction caused by diabetes mellitus. Instead we need long-term observations of spirometry results to diagnose lung microangiopathy. Microangiopathy lung impairment is characterised by a decrease in spirometric parameters FVC (the maximum volume of air that can be exhaled or inspired during a forced manoeuvre) and FEV_1 (the forced expiratory volume during the first second of expiration) (Davis et al, 2004), (Litonjua et al, 2005), (Yeh et al, 2008).
A later study (Kuziemski et al, 2009) proved that a single spirometric test is insufficient to identify lung microangiopathy on account of functional reserve breathing. The reserves compensate, to some extent, the lung dysfunction, and thus the negative effect of diabetes is concealed until the effect reaches a higher level of impairment.
Since the direct measurements of pulmonary function are not conclusive and post-mortem autopsies do not serve the given patient, the diagnostics have to be based on such indirect results as spirometric measurements and modelling. It is probably also capable of revealing lung microangiopathy if the results are very carefully analysed.
Perfusion computed tomography (pCT) is a diagnostic method that enables the imaging of the organ and tissue. This is a powerful tool for diagnosing perfusion of internal organs such as the brain, liver, pancreas, spleen, kidneys and lungs (Alonzi & Hoskin, 2006), (Blomley et al, 1993), (Cao, 2011), (Eichinger et al, 2010), (Kuziemski et al, 2011). The method enables quantitative evaluation of circulation by determining changes in tissue during the flow of a contrast agent in the blood vessels. Changes, when compared to a normal tissue, can indicate tissue pathology. Lung pCT measurements can help in the diagnosis of cystic fibrosis (Eichinger et al, 2010) and diabetes (Kuziemski et al, 2011). It can also help to differentiate benign pulmonary nodules from lung cancer (Alonsi & Hoskin, 2006).
The technique of lung pCT involves the intravenous injection of a non-iodinated contrast agent and the sequential scanning of the diagnosed region of the chest. There are a number of pulmonary perfusion parameters, calculated pixel by pixel on the basis of raw CT data, which are next analysed in order to reveal differences between the normal and altered tissue. The most useful perfusion parameters are: blood volume (BV), blood flow (BF), mean transit time (MTT), time to peak (TTP) and permeability surface (PS) (Kuziemski et al, 2011).
The diagnosis of pulmonary function has to be based on indirect results, such as diffusing capacity, spirometry and pCT because direct assessment is difficult.

2. Materials

The tests were performed on a group of 72 diabetics. People with cardiovascular disease and smokers were not included in this group.
First the diabetics were tested for microangiopathy, by comparing diffusing capacity in standing and lying position, and on this basis they were split into two groups: $M^{angiop} = 44$ and $M^{non-angiop} = 28$, with and without microangiopathy respectively.
The spirometric tests were carried out on all the patients ($M = M^{angiop} + M^{non\text{-}angiop}$) to obtain the following spirometric parameters: FEV_1 (forced expiratory volume during the first second of expiration), FVC (the maximum volume of air that can be exhaled or inspired during a forced manoeuvre), PEF (peak expiratory flow), MEF_{50} (maximal instantaneous forced expiratory flow where 50% of the FVC remains to be expired), $MEF_{75/25}$ (maximal

mid-expiratory flow), IC (inspiratory capacity) and $FEV_1\%FVC$ (percentage relation of FEV_1 to FVC).
The pCT test was performed on a group of 18 subjects: 10 diabetics and 8 non-diabetic volunteers. The local perfusion parameters BF (blood flow), BV (blood volume), MTT (mean transit time) and PS (permeability surface) were obtained in selected regions of interest (ROI) in the artery and parenchyma.
The patients classified as suffering from microangiopathy had breathing impairment symptoms cause only by diabetes. They were all non-smokers and had not been diagnosed with any other acute or chronic respiratory disease.

3. Diffusing capacity

The quality of gas exchange in the lungs depends on the diffusing capacity $D_L[mol \cdot s^{-1} \cdot kPa]$. During the measurement of D_L (American Thoracic Society, 1995) a person takes a full inhalation of air mixed with small amounts of carbon monoxide and helium. The mixture is held in the lungs for a few seconds and then exhaled. The first part of the expired gas is discarded. The next portion, which includes gas from the alveoli, is collected. The D_L is determined by analyzing and comparing the concentrations of carbon monoxide and helium in the samples of the inhaled gas and the exhaled gas. The alveolar volume V_A is also determined in this test by using the single-breath helium dilution technique.

3.1 The oxygen pathway model

Fig. 1 shows oxygen diffusion. Oxygen transportation from the alveoli to erythrocytes, through the alveoli-capillary barrier, is presented as the flow $f_{21}\,[g\,s^{-1}]$. The blood saturation $S \in (0,1)$, (also given as $S \in (0,100\%)$) shows what part (percentage) of oxygen capacity (maximum amount of oxygen transported by the erythrocytes) is currently being transported in the blood. Poorly oxygenated blood enters the pulmonary artery and then, enriched in oxygen, flows out of the lung through the pulmonary vein. Lung arterial blood saturation S_A differs from lung venous blood saturation S_V, $S_A < S_V$.
Flows $f_{20}[g \cdot s^{-1}]$ and $f_{02}[g \cdot s^{-1}]$ represent the amount of oxygen in the blood flowing into the lung and flowing out of the lung. The oxygen diffusion model is:

$$\begin{cases} \dot{m}_1(t) = -f_{21}(t) + u(t), & m_1(0) \\ \dot{m}_2(t) = f_{21}(t) + f_{20}(t) - f_{02}(t), & m_2(0) \end{cases} \tag{1}$$

where the $m_1(t)[g]$ and $m_2(t)[g]$ are the O_2 masses in the alveoli and in the blood vessels respectively. The initial states $m_1(0)[g]$ and $m_2(0)[g]$ depend on oxygen partial pressure $P_1(0) = 13.32\ [\mathrm{k}Pa]$, $P_2(0) = 12.63\ [kPa]$ and region volume $V_1 = V_A$, $V_2 = 10^{-4}[m^3]$, (Dalquen, 1999) ,West, 2008) and (Taylor et al, 1989). The alveolar volume $V_1 = V_A$ is measured during the diffusing capacity test. The relationship between the O_2 mass and the pressure is: $P_i(t) = RTm_i(t)/M_{O_2}V_i$, $i = 1,2$, where $R\ [N\,m\,K^{-1}\,mol^{-1}]$ is gas constant, T is absolute temperature and $M_{O_2}[g\ mol^{-1}]$ is the molecular mass. The mass diffusion, i.e. flow $f_{21}(t)$ via the membrane is caused by the concentration gradient $\Delta c = c_1 - c_2 > 0$, where $c_i(t) = m_i(t)/V_i$, $i = 1,2$:

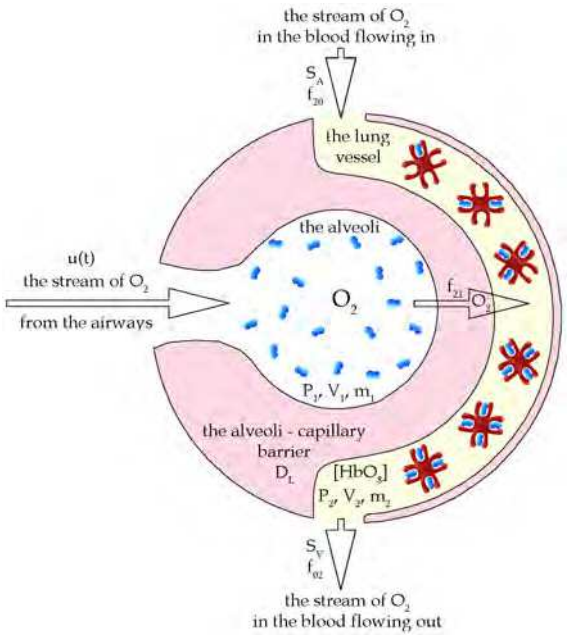

Fig. 1. The passage of oxygen from the airways to the lung vessels. The diffusing capacity D_L describes the condition of the alveoli-capillary barrier. The oxygen is bound in reversible bonds $[HbO_8]$ with the haemoglobin in the lung vessels

$$f_{21}(t) = D_L \cdot R \cdot T \cdot \left(\frac{m_1(t)}{V_1} - \frac{m_2(t)}{V_2} \right) \tag{2}$$

The signal $u(t)$ represents respiratory flow with the period T_p, the delay time t_0 [s] (the time the air passes through the airway to the alveoli) and the duty cycle d. The input amplitude $[g\ s^{-1}]$ depends on the organism's metabolic rate (MR), i.e. the organism's need for oxygen.

In medical practice, blood saturation S gives the basic information concerning the quantity of oxygen transported from the lungs to all the other organs. The kinetics of oxygen association with haemoglobin is described in Hill's equation (Khee-Shing, 2007):

$$S_V(t) = \frac{K \cdot \left(P_2(t)\right)^n}{1 + K \cdot \left(P_2(t)\right)^n} \tag{3}$$

where $P_2(t)$ is oxygen partial pressure in the blood, $n = 2.8$ is the Hill's constant and $K = 1.2256 \cdot 10^{-10}\ [1/(Pa)^n]$ is the association constant. The relationship between the endogenous inflow f_{20} , the outflow f_{02} and the organism's need for oxygen MR is as follows:

$$f_{20}(t) = f_{02}(t) - MR \tag{4}$$

while the outflow f_{02} depends on the blood velocity $\varphi[m^3 s^{-1}]$, maximum erythrocyte oxygen capacity $\Phi[mol \cdot m^3]$ and venous blood saturation $S_V(t)$

$$f_{02}(t) = S_V(t) \cdot \varphi \cdot \Phi \cdot M_{O_2} \tag{5}$$

The elimination flow f_{02}, according to Hill's equation, is:

$$f_{02}(t) = \frac{c_{Hill}}{1 + c_{Hill}} \cdot \varphi \cdot \Phi \cdot M_{O_2}, \quad c_{Hill} = K \cdot m_2^n(t) \cdot \left(\frac{R \cdot T}{M_{O_2} \cdot V_2} \right)^n \tag{6}$$

Taking into account (4), (5) and (6), the oxygen diffusion model is:

$$\begin{cases} \dot{m}_1(t) = -p_1 \cdot m_1(t) + p_2 \cdot m_2(t) + u_1(t), & m_1(0) \\ \dot{m}_2(t) = p_1 \cdot m_1(t) - p_2 \cdot m_2(t) - MR, & m_2(0) \end{cases} \tag{7}$$

where $u_1(t) = \frac{MR}{d} \cdot \sum_{i=0}^{\infty} \left[\mathbf{1}\left(i \cdot T_p - t_0\right) - \mathbf{1}\left(\left(i \cdot T_p - t_0\right) - T_p \cdot d\right) \right]$.

The model parameters $p_1 = D_L \cdot R \cdot T / V_1$ and $p_2 = D_L \cdot R \cdot T / V_2$ can be estimated with the use of measurements D_L, V_1 and physiological constants R, T, V_2.

The example measurements (lying body position), $V_A^{non-\,angiop} = 5.42 \cdot 10^{-3}[m^3]$, $D_L^{non-\,angiop} = 1.54 \cdot 10^{-7}[mol \cdot s^{-1} Pa]$, $V_A^{angiop} = 5.71 \cdot 10^{-3}[m^3]$ and $D_L^{angiop} = 1.59 \cdot 10^{-7}[mol \cdot s^{-1} Pa]$ together with the constants: $V_2 = 0.10 \cdot 10^{-3}\ [m^3]$ (blood volume in lung capillary vessels), $T = 293\ [K]$ (absolute temperature) and $R = 8.314\ [N \cdot m \cdot mol^{-1} K^{-1}]$ (gas constant), allow calculation of the example model parameter estimates:

$$\mathbf{p}^{angiop} = [p_1^{angiop}, p_2^{angiop}] = [5.6315 \cdot 10^{-2},\ 3.3271]$$
$$\mathbf{p}^{non-angiop} = [p_1^{non-angiop}, p_2^{non-angiop}] = [6.2128 \cdot 10^{-2},\ 3.9621]$$

The model parameter estimates have been calculated for all the $M = 72$ patients.

3.2 Statistical comparison of measurement and modelling results for microangiopathic and non- microangiopathic patients

Measurements were made for two groups of diabetic patients: ones with diagnosed microangiopathy and others with no microangiopathy. Lung microangiopathy was identified when $D_L^{\text{standing}} > D_L^{\text{lying}}$. This examination also gives the alveoli volume $V_A = V_1$.

The null hypothesis H_0 assumes that the mean values in both groups of patients are the same. Calculated *ex post* significance level p is compared with *ex ante* significance level α (test-T). If a test of statistical significance gives *ex post* significance level p, which is lower than the α, the null hypothesis is rejected, alternatively we no grounds to reject this hypothesis. Table 1 and Table 2 show a statistical comparison of spirometry measurements and model parameters obtained from microangiopathic and non-microangiopathic patients. The results presented in Table 1 ($H_0: \bar{D}_L^{\text{lying}\,angiop} = \bar{D}_L^{\text{lying}\,non-\,angiop}$ is rejected and the conclusion is: $\bar{D}_L^{\text{lying}\,angiop} \neq \bar{D}_L^{\text{lying}\,non-\,angiop}$) suggest the possibility of diagnosing

microangiopathy on the basis of D_L^{lying} only, instead of D_L^{lying} and D_L^{standing}. The lack of statistical significance for D_L^{standing} means that it is not useful as an individual value for microangiopathy diagnosis.

	Microangiopathic		Non-microangiopathic		Statistical significance level p
	Mean value	Standard deviation	Mean value	Standard deviation	
D_L^{standing}	1.64 10-7	0.14 10-7	1.48 10-7	0.11 10-7	$p \geq 0.05$
V_A^{standing}	5.95 10-3	0.21 10-3	5.65 10-3	0.21 10-3	$p \geq 0.05$
D_L^{lying}	1.35 10-7	0.06 10-7	1.63 10-7	0.14 10-7	$p < 0.05$
V_A^{lying}	6.04 10-3	0.27 10-3	5.90 10-3	0.40 10-3	$p \geq 0.05$

Table 1. Statistical comparison of D_L and V_A. For D_L^{lying} *ex post* significance level is $p < \alpha$, $\alpha = 0.05$. The null hypothesis $H_0: \bar{D}_L^{\text{lying}\,angiop} = \bar{D}_L^{\text{lying}\,non-angiop}$ concerning equality of mean diffusing capacity values in both groups was rejected. D_L^{lying} allows us to distinguish between patients with and without microangiopathy, while the rest do not.

	Microangiopathic		Non-microangiopathic		Statistical significance level p
	Mean value	Standard deviation	Mean value	Standard deviation	
Measurements taken in standing body position					
p_1	$6.6176 \cdot 10^{-2}$	$0.4720 \cdot 10^{-2}$	$6.1900 \cdot 10^{-2}$	$0.2792 \cdot 10^{-2}$	$p \geq 0.05$
p_2	3.9330	0.3447	3.5301	0.2730	$p \geq 0.05$
Measurements taken in lying body position					
p_1	5.4339 10-2	0.2233 10-2	6.5672 10-2	0.3139 10-2	$p < 0.01$
p_2	3.2427	0.1551	4.0981	0.3518	$p < 0.01$

Table 2. Statistical comparison of p_1 and p_2. In the lying body position the ex post significance level is $p < \alpha$, $\alpha = 0.01$ and the H_0, concerning the equality of mean parameter values, is rejected. These parameters allow for a distinction to be made between patients with and without microangiopathy.

Next, the null hypothesis $H_0 = \bar{p}_i^{angiop} = \bar{p}_i^{non-angiop}$, $i = 1,2$ was tested (Table 2). The Kolmogorov-Smirnov test accepted the normality hypothesis concerning p_1 and p_2 at the significance level of $p < 0.01$. Therefore the mean values and standard deviations were calculated and the null hypothesis $H_0 = \bar{p}_i^{angiop} = \bar{p}_i^{non-angiop}$ was tested.

For p_1 and p_2, in lying body position, the *ex post* significance level $p < \alpha$, $\alpha = 0.01$ and so the H_0 was rejected. These parameters enable a distinction to be made between patients with and without microangiopathy.

In a standing body position ($p \geq 0.05$) the parameters p_1 and p_2 are not useful for microangiopathy diagnosis.

The results in Table 1 and Table 2 indicate the possibility of using a diagnostic test based on a single measurement D_L^{lying}, and also on the basis of modelling results p_1 .and p_2.

3.3 Binary classification on the basis of diffusing capacity measurement and modelling

Statistical analyses show that a single measurement D_L^{lying} and the model parameters p_1, p_2 contain information concerning lung microangiopathy. The question remains as to whether or not such values can be used for binary classification. Binary classification is the classifying of the members of mixed group $M = M^{angiop} + M^{non\text{-}angiop}$ into two subgroups, M^{angiop} and $M^{non-angiop}$, on the basis of whether or not they have microangiopathy. For this purpose an appropriate classification algorithm has to be chosen.

To select the best potential classification algorithm, statistical measures, sensitivity and specificity (Panzer, Blach & Griner, 1991) were considered. Sensitivity $Sens$ is the ability of a test to detect a disease when it is really present. Specificity $Spec$ is the ability to confirm the absence of a disease in patients when it is really absent.

$$Sens = \frac{True\ Positive}{True\ Positive + False\ Negative} \tag{8}$$

$$Spec = \frac{True\ Negative}{True\ Negative + False\ Positive} \tag{9}$$

The theoretically optimal prediction is: $Sens = 100\%$ (all the sick patients were identified as sick) and $Spec = 100\%$ (none of the healthy patients was identified as sick).

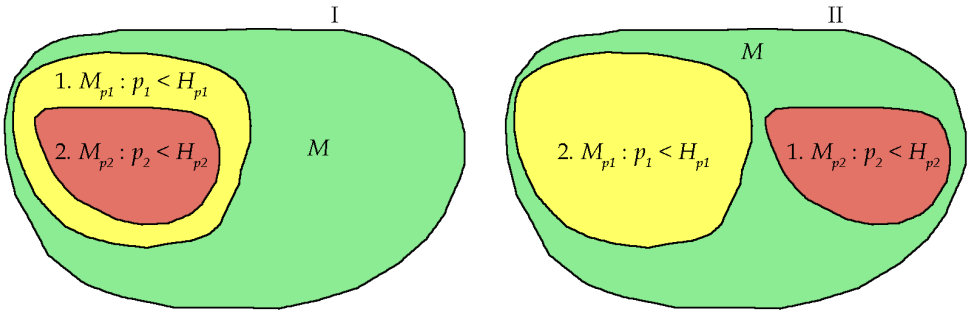

Fig. 2. Classification algorithms based on p_1 and p_2; I) M_{p_2} are classified as microangiopathic and $M - M_{p_2}$ are classified as non-microangiopathic, II) $M_{p_1} + M_{p_2}$ are classified as microangiopathic and $M - (M_{p_1} + M_{p_2})$ are classified as non-microangiopathic

For binary classification the discrimination levels (boundaries, diagnostic thresholds) H_{D_L}, H_{p_1} and H_{p_2} have to be calculated, respectively for D_L, p_1 and p_2. The discrimination levels classify the test result as positive or as negative. The parameter value where $Sens + Spec = \max$ was chosen as the parameter's diagnostic threshold.

Among different classification algorithms using p_1, p_2, H_{p_1} and H_{p_2} the best are the two shown in Fig. 2.

Classification algorithm	Wide range of anthropometric features, $M = 72$ (men and women, 21-69 y, 1.50-1.95m)		Narrowed range of anthropometric features $M_1 = 22$ (women, over 50 y, under 1.65 m)	
	Sens[%]	*Spec*[%]	*Sens*[%]	*Spec*[%]
I. p_1, p_2	50	<u>84</u>	62	<u>87</u>
II. p_2, p_1	<u>76</u>	50	<u>79</u>	80
D_L^{lying}	33	61	62	71

Table 3. Classification results obtained for entire group of $M = 72$ subjects and for the group of $M_1 = 22$ women, over 50 y, under 1.65 m. The best results are underlined.

Therefore the diagnostic procedure shown in Fig. 3 is recommend.

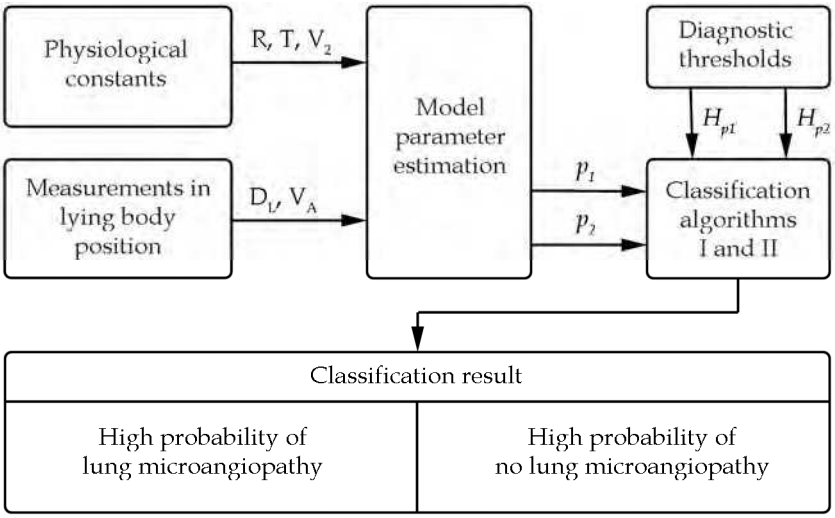

Fig. 3. Diagnostic procedure with the use of D_L^{lying}, V_A^{lying} measurements, constants *R*, *T*, V_2 and calculated p_1, p_2, H_{p_1} and H_{p_2}. For binary classification the more conclusive algorithms I) (with respect to *Spec*) and II) (with respect to *Sens*) are recommended.

The binary classification was performed for the $M = 72$ subjects. The results were compared with already known medical diagnoses of 44 microangiopathic patients and 18 patients with no microangiopathy. Then the sensitivity and the specificity were calculated according to equations (8) and (9), (Table 3). The larger the *Sens* and *Spec* , the better. It seems reasonable to assume that results larger than 75% are satisfactory. Therefore an algorithm should be selected to fulfil this requirement, and not every entry in Table 3 does.

Diagnostic thresholds, calculated on the basis of $M = 72$ measurement data, are: $H_{p_1} = 5.80 \cdot 10^{-2}$, $H_{p_2} = 3.50$ and $H_{D_L} = 1.57 \cdot 10^{-7}$. The best statistical measures obtained are: $Sens = 76\%$ (algorithm II) and $Spec = 84\%$ (algorithm I). The results for D_L^{lying}, $Sens = 33\%$ and $Spec = 61\%$, are less than 75% and quite inadequate.

The thresholds established as common for the entire group did no take into account such important factors as age, height and gender. Therefore a subgroup $M_1 = 22$ was selected (women, over 50 years old and less than 1.65 m tall). Then the new diagnostic thresholds $H_{p_1} = 5.42 \cdot 10^{-2}$, $H_{p_2} = 3.06$, $H_{D_L} = 1.30 \cdot 10^{-7}$ and new *Sens* and *Spec* were calculated. As expected, both the new *Sens* and *Spec* were noticeably larger.

The diagnostic procedure in Fig. 3 uses D_L^{lying} and V_A^{lying} measurements, and R, T and V_2 physiological constants to calculate the p_1 and p_2 in a patient. Then algorithm I (with the most conclusive *Sens*) and algorithm II (with the most conclusive *Spec*) are applied together with H_{p_1} and H_{p_2} diagnostic thresholds to obtain a binary classification result.

This procedure produces one of two possible results: 1) high probability of lung microangiopathy or 2) high probability of no lung microangiopathy. This can serve as useful confirmation in a doctor's diagnosis.

The final decision is made by the doctor conducting the diagnosis, who can take into account this classification result along with other diagnostic data.

4. Spirometry

The most popular spirometry method is a dynamic one. The pneumotachometer (Miller, Harkinson&Brusasco, 2005) defines the volume $V(t)$ [l] and airflow $Q(t)$[ls^{-1}] during the inhalation and exhalation. The flow-volume curve $Q(V)$ is received on the basis of the spirometry measurements of $V(t)$ and $Q(t)$. Specific ventilation manoeuvres are required in the spirometric test. The measurement is preceded by a period of quiet breathing–in and out (Fry, Hyatt, 1960). Next the maximal breath–in and the maximal forced breath–out manoeuvres are performed as the important parts of the spirometric test.

The respiration parameters are defined on the basis of the volume–time curve $V(t)$ and the flow–volume curves $Q(V)$ (see Fig. 4 and Fig. 5), (Miller, Harkinson&Brusasco, 2005).

In medical practice two terms, volume and capacity, are used. The difference between them is based on the assumption that volume refers to lung volumes, while capacity refers to different combinations of lung volumes, usually in relation to inhalation and exhalation.

The relations between volumes and capacities are presented in equations (10).

$$\begin{aligned} TLC &= VC + RV \\ TLC &= IC + FRC \end{aligned} \tag{10}$$

The following respiratory parameters have been defined: TLC [l] (Total Lung Capacity) is the volume of air in the lungs at the end of maximal inhalation; VC [l] (Vital Capacity) is the maximum volume of air that can be exhaled or inhaled during either a forced (FVC) or a slow (VC) manoeuvre; RV [l] (Residual Volume) is the volume of air remaining in the lungs after the maximal exhalation; IC [l] (Inspiratory Capacity) is the maximal volume of air that can be inhaled from the resting expiratory level; FRC [l] (Functional Residual Capacity) is the volume of air in the lungs at the resting end-expiration.

Also defined are the following respiratory parameters: FEV_1 [l] the forced expiratory volume during the first second of expiration; FET [s] the forced expiratory time; FIT [s] the forced inspiratory time; PEF [$l\ s^{-1}$] (Peak Expiratory Flow) and PIF [$l\ s^{-1}$] (Peak Inspiratory Flow) are respectively the maximal expiratory and the maximal inspiratory flow

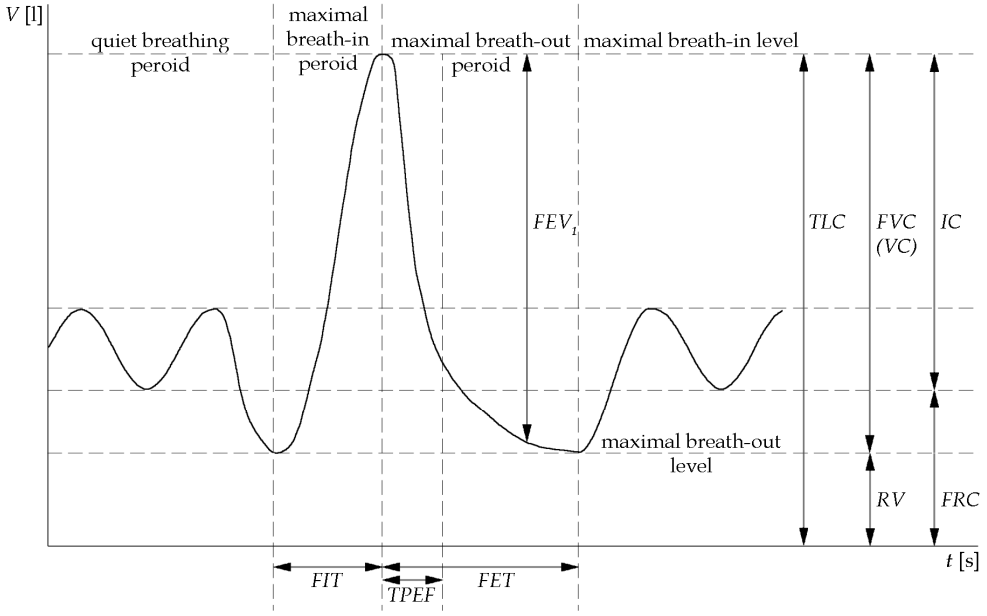

Fig. 4. The spirometry parameters defined on the basis of volume-time curve $V(t)$.

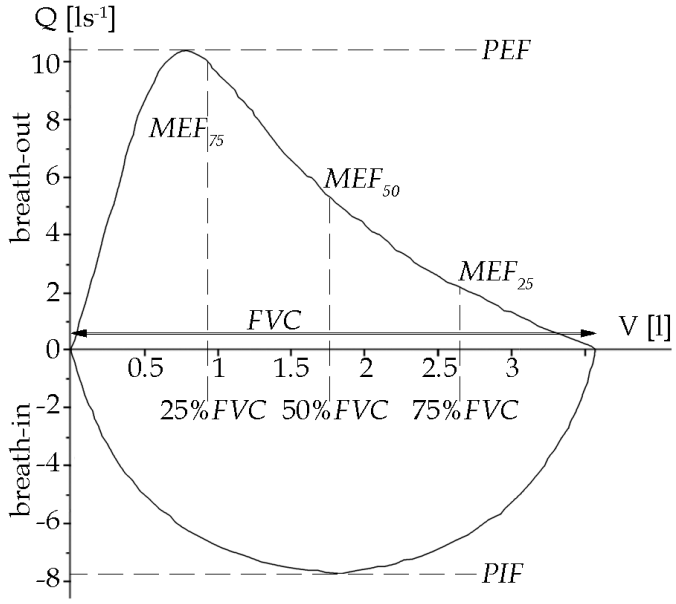

Fig. 5. The spirometric parameters defined on the basis of flow–volume curve $Q(V)$.

rates achieved; $TPEF$ $[s]$ the time of maximal expiratory flow; $MEF_{75}, MEF_{50}, MEF_{25}$ $[l\,s^{-1}]$ maximal instantaneous forced expiratory flow where 75, 50, 25% of the FVC remains to be expired; $MEF_{75/25}$ $[l\,s^{-1}]$ is the maximal mid-expiratory flow and $FEV_1\%FVC$ is the percentage relation of FEV_1 to FVC.

The European Respiratory Society (Miller, Harkinson & Brusasco, 2005) has published the spirometric norms and the reference values for these spirometric parameters. The reference values of the respiration parameters, obtained for a representative healthy population, are used for the interpreting the spirometry data and making the diagnosis. The reference values depend on the patient's anthropometric data, such as age, height and gender. In some medical cases (asthma, pulmonary fibrosis, cystic fibrosis and COPD) the spirometric parameter boundary values have already been defined. However, as far as lung microangiopathy is concerned, this has not yet been done.

According to medical practice experience, lung microangiopathy is diagnosed on the basis of the following spirometric parameters: FEV_1, FVC, PEF, MEF_{50}, $MEF_{75/25}$, IC and $FEV_1\%FVC$. These spirometric parameters were collected from the $M = 72$ diabetic patients. However, a single spirometric test is not sufficient to diagnose the lung flow and volume reduction caused by microangiopathy; long term observation is necessary. Therefore one should consider an alternative method. By using the spirometric results in a statistical significance test, we can find the spirometric parameters that are most responsive to lung microangiopathy.

4.1 Spirometric parameters. Statistical comparison of results for microangiopathic and non- microangiopathic patients

Traditional spirometric parameters were tested for their ability to detect lung microangiopathy. The mean, standard deviation and the statistical significance level p for spirometric parameters are presented in Table 4.

	Microangiopathic		Non-microangiopathic		Statistical significance level p
	Mean spirometry parameter	Standard deviation	Mean spirometry parameter	Standard deviation	
FEV_1	2.970	0.699	2.919	0.832	$p \geq 0.05$
FVC	4.245	0.911	4.015	1.245	$p \geq 0.05$
PEF	9.175	1.545	11.621	1.914	$p \geq 0.05$
MEF_{50}	5.258	1.384	3.691	1.637	$p \geq 0.05$
$MEF_{25/75}$	2.896	1.051	2.853	1.206	$p \geq 0.05$
IC	3.182	0.706	3.275	1.097	$p \geq 0.05$
$FEV_1\%FVC$	70.731	7.482	73.621	8.880	$p \geq 0.05$

Table 4. Statistical comparison of spirometric parameters for microangiopathic and non-microangiopathic patients. In every case the *ex post* significance level $p > \alpha$, $\alpha = 0.05$, which means that H_0 concerning mean parameter value equality is not rejected. The parameters do not allow for a distinction to be made between patients with and without microangiopathy.

The parameters do not show statistical significance in detecting microangiopathy: *ex post* significance level p is larger than *ex ante* significance level $\alpha = 0.05$, which confirms the null hypothesis concerning equality of mean values for both groups. Therefore, none of spirometric parameters are useful in diagnosing microangiopathy.

4.2 Spirometry modelling

The maximal breathing-in flow was modelled by means of the sine function. The forced breathing-out flow was finally mimicked using the gamma variate function (Askey R.A.& Roy R,2007) – after testing a large group of prospective regression functions, such as exponentials, polynomials, etc (Kalicka et al, 2007).
The maximal inflow $Q_{in}(V)$ is modelled as follows:

$$Q_{in}(V) = A_{in} \cdot \sin(\varpi \cdot V),\ 0 \le V \le FVC \tag{11}$$

where A_{in} [$l\ s^{-1}$] and ϖ [l^{-1}] are model parameters and FVC is the forced vital capacity.
For modelling $Q_{out}(V)$ during the maximal outflow, the following gamma variate function is implemented:

$$Q_{out}(V) = K(V)^{b} e^{-V \cdot a},\ FVC \ge V \ge 0 \tag{12}$$

where K[$l\ s^{-1}$], b and a [l^{-1}] are model parameters.
The model consists of the equations (11) and (12). The model parameters are arranged into vector $\mathbf{p} = [p_i] = [A_{in}, \varpi, K, b, a]$, $i = 1 \div 5$. The parameter estimates were obtained using the least square procedure, according to the following:

$$\mathbf{p} = \arg\left[\min_{\mathbf{p}} \sum_{V=0}^{V_{\max}} \left(Q^{\text{model}}(V, \mathbf{p}) - Q^{\text{meas}}\left(V, \mathbf{y}^{\text{meas}}\right) \right)^2 \right] \tag{13}$$

where $\mathbf{y}^{\text{meas}} = [y_j^{\text{meas}}] = [FEV_1, FVC, PEF, MEF_{50}, MEF_{25/50}, IC, FEV\%FVC]; j = 1 \div 7$ is vector of measurements and $V_{\max} = FVC$. The fitting procedure was executed separately to obtain A_{in}, ϖ and K, b, a based on the equations (11) and (12) respectively.
The parameter vector $\mathbf{p} = [A_{in}, \varpi, K, b, a] = [3.780, 1.030, 20.580, 0.772, 1.507]$ is an example of the model identification results. This was obtained from a 59-year-old woman suffering from lung microangiopathy. The spirometric parameters obtained from the patient were: $FEV_1 = 2.25$, $FVC = 2.84$, $PEF = 5.79 l/s$, $MEF_{50} = 3.47 l/s$, $MEF_{75/25} = 2.63 l/s$, $IC = 2.81$ and $FEV_1\%FVC = 78.95\%$.
Calculations of $\mathbf{p} = [A_{in}, \varpi, K, b, a]$ were performed for $M = 72$ diabetic patients. Fig. 6 shows an example of the model regression functions $Q_{in}(V)$ and $Q_{out}(V)$ drawn for the $\mathbf{p} = [A_{in}, \varpi, K, b, a] = [3.780, 1.030, 20.580, 0.772, 1.507]$. In Fig. 6 the $Q(V)$ spirometric test results have been added, for comparison.

4.3 Statistical comparison of modelling results for microangiopathic and non-microangiopathic patients

The mean parameter value and standard deviation were calculated separately for microangiopathic and non-microangiopathic patients (Table 5). The aim was to find out

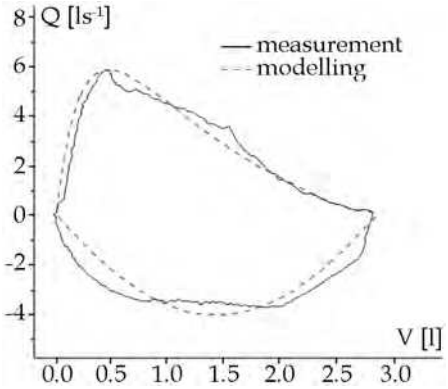

Fig. 6. An example result of the spirometric measurement and modelling of the flow–volume curve $Q(V)$.

	Microangiopathic		Non-microangiopathic		Statistical significance level p
	Mean model parameter	Standard deviation	Mean model parameter	Standard deviation	
A_{in}	5.92	1.72	5.88	2.20	$p \geq 0.05$
ϖ	0.78	0.17	0.82	0.22	$p \geq 0.05$
K	34.79	6.84	53.78	7.56	$p < 0.05$
b	1.193	0.83	1.58	1.06	$p \geq 0.05$
a	1.501	0.59	1.85	0.78	$p < 0.05$

Table 5. Statistical comparison of model parameters for microangiopathic and non-microangiopathic patients. For A_{in}, ϖ and b, the *ex post* significance level was $p > \alpha$, $\alpha = 0.05$, and thus the H_0, concerning mean parameter values equality, was not rejected – i.e. the parameters are not useful for diagnosis. However, parameters K and a are useful in distinguishing between patients with and without microangiopathy because the *ex post* significance level is $p < \alpha$, $\alpha = 0.05$.

whether or not the model parameters are helpful in distinguishing between microangiopathic and non-microangiopathic patients. For this purpose the null hypothesis $H_0 = \overline{p}_i^{angiop} = \overline{p}_i^{non-angiop}$, $i = 1,..,5$ was tested.

At first the normality hypothesis concerning the parameter estimates p_i was investigated, and the hypothesis was accepted (Kolmogorov-Smirnov test) at the significance level of $p < 0.05$. Then the mean values and standard deviations (Table 5) were calculated and statistical test-T was performed. For K and a the *ex post* significance level $p < \alpha$, $\alpha = 0.05$ and H_0 is rejected. The two model parameters K and a allow for a distinction to be made between patients with and without microangiopathy.

The remaining model parameters A_{in}, ϖ and a do not reveal the occurrence or absence of lung microangiopathy.

4.3 Binary classification on the basis of spirometric measurements and modelling

Binary classification algorithms, based on the model parameters K and a, were tested with discrimination levels H_K and H_a. The discrimination levels were first established for all $M = 72$ subjects as $H_K = 50.18$ and $H_a = 1.72$. These discrimination levels correspond to the K and a values for which $Sens + Spec = \max$. The $M = 72$ subjects were now divided into two groups on the basis of these discrimination thresholds.

Two algorithms, I and II (which gave the best results), were applied for binary classification. The algorithms are presented in Fig. 7. The binary classification decision was compared with previously known medical diagnoses, and then the $Sens$ and $Spec$ were calculated according to equations (8) and (9), (see Table 6).

None of the tested algorithms could produce simultaneously a large $Sens$ and a large $Spec$. Algorithm II gave the best $Sens = 82\%$ and algorithm I gave the best $Spec = 62\%$. Algorithm II accurately detected the majority of the microangiopathy cases ($Sens = 82\%$), and only missed out on a few. Yet $Spec = 50\%$ means algorithm II identified only 50% of the non-microangiopathic patients as non-microangiopathic and gave too many false alarms. This is an unacceptable result. Somewhat better $Spec = 62\%$ was obtained with algorithm I but this was still not satisfactory. The most likely explanation for these poor results is the fact that the thresholds H_K and H_a are too general and do not take into consideration important anthropometric features.

Therefore the range of anthropometric features was made more specific ($M_1 = 22$ women, over 50 years old and under 1.65 m tall) and new diagnostic thresholds were calculated: $H_K = 48.11$ and $H_a = 1.68$. The new classification results are presented in Table 6.

This more accurate choice of the diagnostic thresholds gave much better results. The $Sens = 100\%$ means that algorithm II identified all the sick patients as sick. This excellent result has been obtained for the sample $M_1 = 22$ selected from the general population and therefore should be treated with care. An another sample may give a somewhat different result but the great improvement is obvious.

The diagnostic procedure, utilising the algorithms I and II, is shown in Fig. 8.

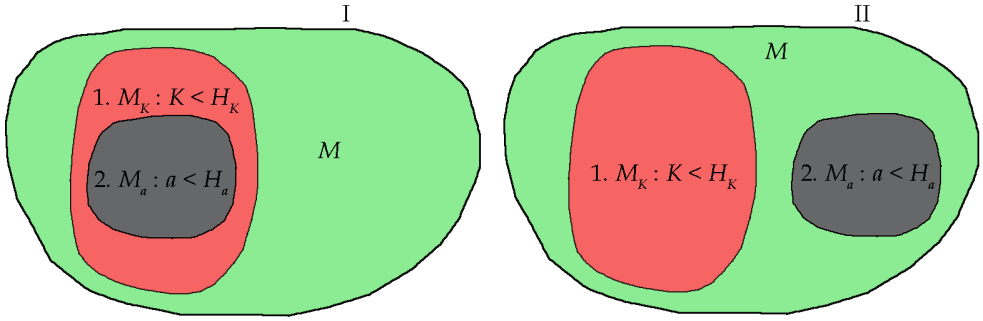

Fig. 7. Classification algorithms based on a and K; I) M_K are classified as microangiopathic and $M - M_K$ are classified as non-microangiopathic, II) $M_a + M_K$ are classified as microangiopathic and $M - (M_a + M_K)$ are classified as non-microangiopathic

Classification algorithm	Full range of anthropometric features, $M = 72$ (men and women, 21-69 y, 1.50-1.95m)		Limited range of anthropometric features $M_1 = 22$ (women, over 50 y, under 1.65 m)	
	Sens[%]	*Spec*[%]	*Sens*[%]	*Spec*[%]
I. a, K	64	<u>62</u>	87	<u>83</u>
II. K, a	<u>82</u>	50	<u>100</u>	80

Table 6. Classification results obtained for entire group of $M = 72$ subjects and for the subgroup $M_1 = 22$ of women over 50 years old and under 1.65 m. The best results are underlined.

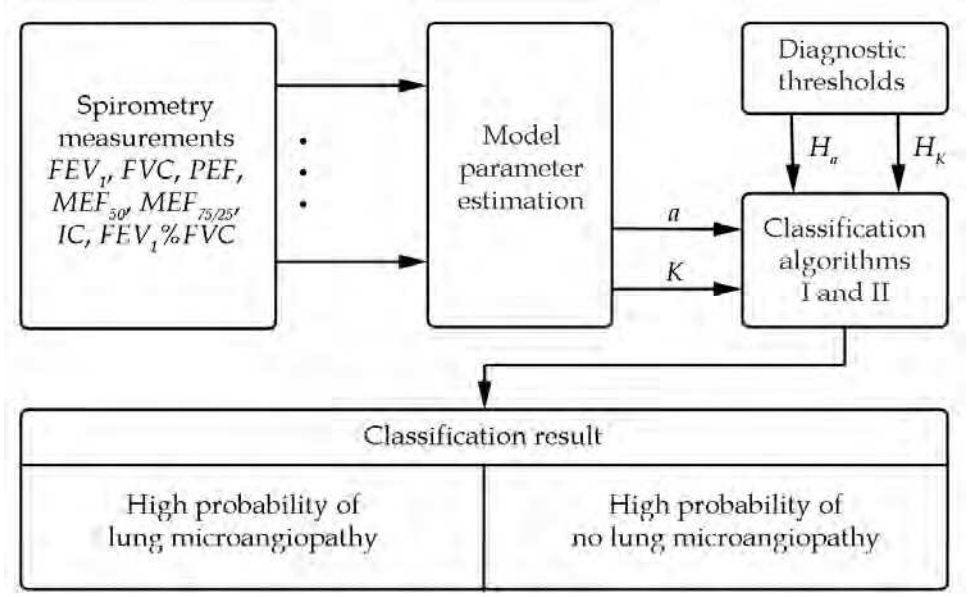

Fig. 8. Classification algorithms: I) M_K are classified as microangiopathic and $M - M_K$ as non-microangiopathic, II) $M_a + M_K$ are classified as microangiopathic and $M - (M_a + M_K)$ as non-microangiopathic

Applied with H_a and H_K, algorithm I gives the best (most conclusive) *Sens* classification result, while the algorithm II gives the best (most conclusive) *Spec* result.
This procedure gives one of two alternative results: 1) high probability of lung microangiopathy or 2) high probability of no lung microangiopathy. The final decision is made by the doctor.

5. Perfusion computed tomography (pCT)

Tests commonly used in clinical practice such as spirometry and lung diffusion capacity measurements are not considered precise enough to identify lung microangiopathy. There are very few publications in this field and most of them concern the decrease of diffusion

capacity in diabetics (Villa et al, 2004), (Goldman, 2003). Autopsies of patients who died of diabetes complications revealed a thickening in the basement membrane of alveolar capillaries and arterioles in the lungs as well as of the entire walls of pulmonary arterioles together with fibroblast proliferation (Weynand et al, 1999).
Impaired gas exchange in pulmonary alveoli results in the progressive reduction of reserves in small pulmonary vessels. For this reason lung perfusion in regions of lung microangiopathy may be diminished. Computed tomography of chest perfusion allows imaging of pulmonary vessels and parenchyma and may be useful in diagnosing pulmonary microangiopathy (Kuziemski et al, 2011).

5.1 Patients and study protocol

A group of 10 never-smoking diabetic adults and a control group of 8 non-diabetic volunteers were chosen. All participants had a similar body mass index and none of them suffered any disease that affected pulmonary function. The mean time from when diabetes mellitus was first diagnosed was 15.5 years. Nephropathy was diagnosed in 3 diabetics, retinopathy in 6 and polyneuropathy in 4. The question was whether or not they also suffered from lung microangiopathy. In the control group lung and cardio-vascular diseases were not diagnosed.
For all patients, spirometry and diffusing capacity tests were performed.
For the pCT tests a 64-row CT scanner GE - Light Speed VCT (GE Healthcare USA) was used. Pulmonary perfusion was evaluated after the intravenous administration of 40 ml of contrast at the rate of 4 ml/s. CT images were taken with 1 s resolution in the period of 40 s of a selected lung section (4 cm thick layer situated 2 cm below carina). Within this 4 cm thick segment, three cross-sections, anterior, medium and posterior, 5 mm thick each, were selected at uniform distances from each other. 6 ROIs were chosen in each of the cross-sections (18 ROIs in all, numbered ROI 3-ROI 20). The ROIs 3–20 were situated in the upper, medial and lower parts of the left and right lungs. The most vascularised areas of the lungs were left beyond the ROIs so as not to distort the evaluation of lung parenchyma.
The pCT measurements were performed using standard CT Perfusion 4 (GE Healthcare USA). The following perfusion parameters were calculated:

- $BV[ml/100g]$ - blood volume in 100g of lung tissue.
- $BF[ml/100g/\text{min}]$ - blood flow through 100g of lung tissue in 1 minute.
- $MTT[\text{min}]$ - mean transit time through the vascular system in selected region.
- $PS[ml/100g/\text{min}]$ - permeability surface, the permeability of blood from intravascular to extravascular space, observed in 100g of lung tissue during 1 min.

5.2 pCT results

The example results of pCT scans, obtained from a 62 year old diabetic male, are shown in Fig. 9 a), b), c) and d). Perfusion parameters BF, BV, MTT and PS were calculated and mapped out on the lung cross-section. Analysis was made of the pulmonary artery - ROI 1, which represents the arterial input function, i.e. the flow blood into the pulmonary system.
In Fig. 9 the ROI 1 is marked with a circle. The calculated values of perfusion parameters (mean value for all pixels in the region and standard deviation of the mean) are displayed in the right lower corner of the scan.
Table 7 shows mean perfusion parameters Avg and standard deviation Dev in the ROI 1.

As the table shows, the obtained permeability surface *PS* for the impermeable pulmonary artery is equal to zero. The *Dev*, i.e. the disperse of parameter values within the ROI 1, is low, 4-7%.

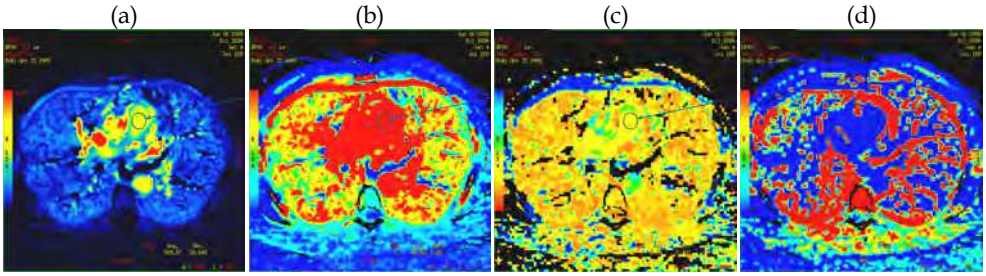

Fig. 9. The pCT scans (a) blood flow BF, (b) blood volume BV, (c) mean transit time MTT and (d) permeability surface PS for a 62 year old diabetic male.

Blood Flow *BF*		Blood Volume *BV*		Mean Transit Time *MTT*		Permeability Surface *PS*	
Avg	*Dev*	*Avg*	*Dev*	*Avg*	*Dev*	*Avg*	*Dev*
509.9	20.64	48.06	3.48	5.65	0.30	0	0

Table 7. Example results of perfusion parameters calculated as the mean values in the ROI 1 marked in Fig. 9. The calculated standard deviations *Dev* illustrates the distribution of test results within ROI 1.

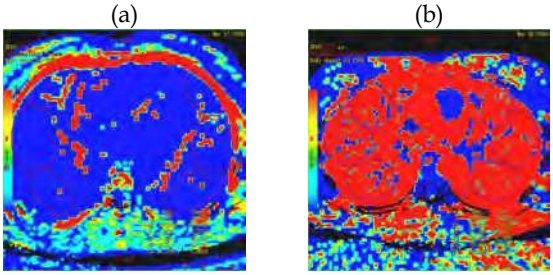

Fig. 10. The PS maps for (a) healthy subject and (b) diabetic subject. For example, in ROI 13 (right lower circle) $PS = 3.31$ for the healthy subject and $PS = 79.80$ for the diabetic subject. The measurements were obtained in the same location of the lung cross-section.

Fig. 10 shows PS maps obtained from a healthy patient and a diabetic patient. The qualitative comparison (amount of the red, permeable area) as well as the quantitative comparison (healthy patient $PS = 3.31$ and diabetic patient $PS = 79.80$) indicate damage to capillaries and pulmonary arterioles of the diabetic patient.
All perfusion parameters were calculated in 18 ROIs (3-20) in the parenchyma to discover whether parameter values depend on the location of tested lung cross-section. Statistical analysis revealed no correlation between perfusion parameter value and ROI location in the upper central or lower part of the lungs (Kuziemski et al, 2011). Therefore mean perfusion

parameters were calculated for all 18 ROIs. The results are shown in Table 8 (Kuziemski et al, 2011).
Here a noticeable increase was observed in the parenchyma perfusion parameter values of the diabetics with respect to control group, which may be due to diabetic mellitus.

$BF[ml/100g/\min] \pm Dev$		$BV[ml/100g] \pm Dev$		$PS[ml/100g/\min] \pm Dev$
Artery	Parenchyma	Artery	Parenchyma	Parenchyma
Diabetes 722.5±301.8	Diabetes 282.2±115.0	Diabetes 62.8±25.2	Diabetes 16.2±6.4	Diabetes 35.6±26.1
Control 681.7±133.2	Control 207.6±53.4	Control 61.0±5.9	Control 12.0±1.8	Control 8.6±4.8

Table 8. Mean parameters BF, BV and PS in the artery and parenchyma of the diabetics and of the control group. The calculated standard deviation Dev illustrates the distribution of test results in 18 ROIs (ROI 3 – 20, in upper, central and lower part of lungs) with respect to the mean of the eighteen results. No significant MTT differences were found.

Chest perfusion CT allows imaging of lung vessels and parenchyma, which is essential in diagnosing pulmonary angiopathy. The analyzed results are very new and currently not all that numerous. While this does not allow for a complex statistical analysis, the above preliminary results indicate the great potential of pCT tests in diagnosing lung microangiopathy.

5.3 Lung area extraction

Each pCT image (see Fig. 9) consists of the body cross-section, including the lungs, essential for medical diagnosis, the rest of the body and the background, which is unnecessary for lung diagnostics but was nevertheless included in the perfusion map calculations.
As computations of perfusion parameters involve complicated methods of signal processing, it is desirable that the distinction between diagnostically important regions (the lung cross-section) and other areas (background and the rest of body cross-section) is conducted before the process starts. This shortens the time needed to obtain parametric maps by omitting data processing from the area outside the lungs. It can also help avoiding false lung malfunction diagnoses, which can occur when the automatic methods of pathological changes wrongly interpret signals from areas outside the lungs as abnormal lung signals.
Literature describes many methods of lung area extraction from CT chest scans (Homma et al, 2009), (de Nunzio et al, 2011), (Vinhais & Campilho, 2006), (Zhou et al, 2004). Most methods are devoted to extracting the lung area from a single image. Some of these methods allow for neighbouring (upper and lower) slices to be analysed (Homma et al, 2009).
The lung extraction presented here was obtained using the two-step procedure. The objective of the preliminary processing was to define the rough mask, i.e. the border within which the lung contour is always contained during the pCT test while the lungs are breathing and the heart is beating. The lung and heart region contour pixels are subjected to the greatest changes. This behaviour can be utilised to detect the contours. It can be achieved by using a variability factor VF, which is defined as follows:

$$VF = \frac{x_{\max} - x_{\min}}{x_{median}} \tag{14}$$

where $x_{\max}$, $x_{\min}$ and x_{median} are respectively each pixel's maximum, minimum and median value. VF can be used to create a variability map, M_{VF}. Such a map is shown in Fig. 11.

Fig. 11. Map M_{VF} of variability factor VF. The white areas are the most variable due to the breathing lungs and beating heart.

Then the final lung mask was obtained with the use of morphological operators (dilation, erosion, closing and opening) to extract lung cross-sections from the chest pCT.
Fig. 12 shows the BF, BV, MTT and PS maps of just the lungs, extracted using the mask. The lung mask was superimposed onto the calculated maps in Fig. 9.

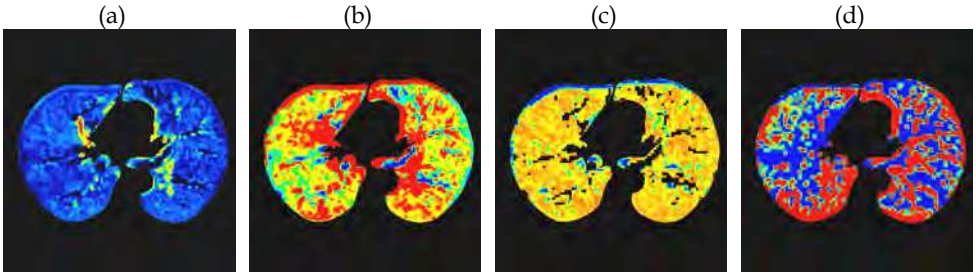

Fig. 12. Lung extraction. The pCT lung maps obtained for the scans in Fig. 9 - (a) blood flow BF, (b) blood volume BV, (c) mean transit time MTT and (d) permeability surface PS.

Visual comparison of Fig. 9 and Fig. 12 shows just how much unnecessary computations are usually performed in areas outside the lungs. What is more, a clearly defined lung area allows for a much more accurate and reliable medical diagnosis.

6. Conclusion

Pulmonary diabetic microangiopathy has not yet been sufficiently studied and is difficult to diagnose. In clinical practice, lung microangiopathy is diagnosed by comparing two diffusing capacity measurements, taken with the patient standing up and lying down. Other methods to assist diagnosis of lung microangiopathy are needed.

The three methods presented here seem good enough to be competitive options to complement those currently used in medicine today.

Diffusing capacity measurement and modelling allows for the development of a procedure to enhance the diagnostic process. This procedure is based on a single diffusing capacity measurement taken from a patient lying down, together with a model of oxygen diffusion from the alveoli to the blood. The model parameters, calculated using routine medical test results and physiological constants, turned out to be useful for binary classification in lung microangiopathy diagnosis. Diagnostic thresholds were calculated. Next binary classification was performed, based on model parameters, and, for comparison, on the diffusing capacity test result. These results were compared with already known medical diagnoses. This allowed for the sensitivity and specificity to be calculated. The best binary classification results were $Sens = 79\%$ and $Spec = 87\%$, when based on model parameters, and, when based on diffusing capacity measurements, $Sens = 62\%$ and $Spec = 71\%$. These results show that for microangiopathy diagnosis the model parameters were more sensitive and more specific than the diffusing capacity measurements.

The next method to be examined for usefulness in lung microangiopathy diagnosis was spirometry. Statistical comparison of the spirometry parameters of microangiopathic and non-microangiopathic patients, revealed that such parameters do not allow for a distinction to be made between patients with and without microangiopathy. Therefore a spirometry model was developed and its parameters were tested for their ability to distinguish between microangiopathic and non-microangiopathic subjects. Two, out of five, model parameters were statistically significant and helpful in lung microangiopathy diagnosis. Diagnostic thresholds were calculated and binary classification was performed, based on the statistically significant model parameters. The best results were $Sens = 100\%$ and $Spec = 83\%$.

Both diagnostic procedures, the one based on the diffusing capacity and the one based on spirometric measurements and modelling, produce one of two possible results: 1) high probability of lung microangiopathy or 2) high probability of no lung microangiopathy.

Perfusion CT measurement seems to have considerable diagnostic potential with regard to lung microangiopathy. A study of lung tissue perfusion in diabetic patients in comparison with a group of healthy subjects showed an increase in the value of some parameters. These increased values may result from pulmonary microangiopathy. Further studies on the application of pCT in the detection of diabetes mellitus may not only improve diagnosis but also help us better understand pulmonary microangiopathy.

7. References

Alonzi R. & Hoskin P. Functional Imaging in Clinical Oncology: Magnetic Resonance Imaging- and Computerised Tomography-based Techniques, *Clin. Oncol*., 18, 7, pp. 555-570, 2006

American Thoracic Society: Single-breath carbon monoxide diffusing capacity (transfer factor): recommendations for a standard technique - 1995 update. *Am. J. Respir. Crit. Care Med*.;152:2185-2198, 1995

Askey R.A., Roy R. Gamma function. In: *Digital Library of Mathematical Functions*. Edited by Olver FWJ, Lozier DM, Boisvert RF., N.I.S.T., 2007

Blomley M.J., Coulden R., Bufkin C., Lipton M.J.& Dawson P. Contrast bolus dynamic computed tomography for the measurement of solid organ perfusion. *Invest. Radiol*., 28, pp. 72-77, 1993

Cao, Y. The Promise of Dynamic Contrast-Enhanced Imaging in Radiation Therapy, *Semin. Radiat. Oncol*.,21, 2, pp. 147-156, 2011

Dalquen, P. The lung in diabetes mellitus, *Respiration, International Journal of Thoracic Medicine*, Vol.66, No1, 1999

Davis A.W., Knuiman M., Kendall. P, Grange V. & Davis T. Glycemic exposure is associated with reduced pulmonary function in type 2 diabetes. *The Fremantle Diabetes Study. Diabetes Care*, 27:752–757, 2004

Eichinger M., Heussel C-P., Kauczor, H-U., Tiddens, H. & Puderbach, M. Computed Tomography and Magnetic Resonance Imaging in Cystic Fibrosis Lung Disease. *Jour. Magn. Reson. Imaging*., 32, pp. 1370–1378, 2010

Fry D.L., Hyatt R.E. Pulmonary mechanics: a unified analysis of the relationship between pressure, volume and gas flow in the lungs of normal and diseased human subjects. Am. J. Med. 29:672-689,1960

Goldman D. Lung dysfunction in diabetes. *Diabetes Care*.;26:1913–1918, 2003

Kalicka R., Słomiński W.& Kuziemski K. Modelling of spirometry. Diagnostic usefulness of model parameters. *The IEEE Eurocon Conference*, 2137-2143, Warsaw 2007

Kaminski D., Spirometry and diabetes: Implications of reduced lung function. Diabetes Care; 27:837–838, 2004

Khee-Shing ML. Configuration of the haemoglobin oxygen dissociation curve demystified: a basic mathematical proof for medical and biological sciences undergraduates. *Advan Physiol Educ*.;31:198-201, 2007

Kida K., Utsuyama M., Takizawa T. & Thurlbeck W. Changes in lung morphologic features and elasticity caused by streptozotocin-induced diabetes mellitus in growing rats *Am. Rev. Respir. Dis*. 128:125–131, 1983

Kodolova I.M., Lysenko L.V.&Saltykov B.B. Changes in the lungs in diabetes mellitus. Arkh. Patol., 44:35-75, 1982

Kuziemski K., Górska L., Jassem E.& Madej-Dmochowska A. Lung microangiopathy in diabetes. *Pneumonol. Alergol. Pol*.;77:394-399, 2009

Kuziemski K., Górska L., Słomiński W., Kalicka R., Specjalski K.& Adamczyk-Bąk K., Sensitivity of DLCO for microangiopathy diagnosis. *Pneunomol. Alergol. Pol*. 76:43A, 2008

Kuziemski K., Pieńkowska J., Słomiński W., Specjalski K., Dziadziuszko K., Jassem E., Studniarek, M. Kalicka, R. & Słomiński J.M. Role of quantitative chest perfusion computed tomography in detecting diabetic pulmonary microangiopathy. *Diabetes Res. Clin. Pr*., 91, pp. 80-86, 2011

Litonjua A., Lazarus R., Sparrow D., DeMolles D. & Weiss S: Lung function in type 2 diabetes: the Normative Aging Study. *Respir. Med*. 99:1583–1590, 2005

Matsubara T.& Hara F. The pulmonary function and histological studies of the lung in diabetes mellitus. *Journal of Nippon Medical School*;58:528–536, 1991

Miller M.R., Hankinson J. & Brusasco V. Standardisation of spirometry. *Eur. Respir. J.* 26:319-338, 2005

Panzer R.J., Black E.R. & Griner PF. Diagnostic strategies for common medical problems. Philadelphia: American College of Physicians, 1991

Popov D, Simionescu M. Alterations of lung structure in experimental diabetes, and diabetes associated with hyperlipidaemia in hamsters. *Eur. Respir. Journal*.;10:1850–1858, 1997

Strojek K., Ziora D., Sroczyński J.& Oklek K. Late lung symptoms of diabetes. *Pneunomol. Alergol. Pol*. 61:166, 1993.

Taylor AE, Rehder K, Hyatt RE & Parker JC. Clinical Respiratory Physiology. Emeryville: W.B.Saunders Company, 1989

Villa M.P., Montesano M., Barreto M., Pagani J., Stegagno M. & Multari G. Diffusing capacity for carbon monoxide in children with type 1 diabetes. *Diabetologia*; 47:1931–5, 2004

West JB., Respiratory physiology - the essentials. Philadelphia: Lippincott Williams & Wilkins, 2008

Weynand B., Jonckheere A. Frans &, Rahier J. Diabetes mellitus induces a thickening of the pulmonary basal lamina. *Respiration, International Journal of Thoracic Medicine*. 66:14–19, 1999

Yeh H., Punjabi N.M. & Wang N. Cross-sectional and prospective study of lung function in adults with type 2 diabetes: The Atherosclerosis Risk in Communities (ARIC) Study. *Diabetes Care*; 31:741–746, 2008

Homma, N., Shimoyama, S., Ishibashi, T., and Yoshizawa, M.: Lung Area Extraction from X-ray CT Images for Computer-aided Diagnosis of Pulmonary Nodules by using Active Contour Model, WSEAS Trans. Inf. Sci. Appl., 5, 6, pp. 746-755, 2009

de Nunzio, G., Tommasi, E., Agrusti, A., Cataldo, R., de Mitri, I., Favetta, M., Maglio, S., Massafra, A., Quarta, M., Torsello, M., Zecca, I., Bellotti, R., Tangaro, S., Calvini, P., Camarlinghi, N., Falaschi, F., Cerello, P., and Oliva, P.: Automatic Lung Segmentation in CT Images with Accurate Handling of the Hilar Region, *J. Digit. Imaging*, 24, 1, pp. 11-2, 2011

Vinhais, C., and Campilho, A.: Lung Parenchyma Segmentation from CT Images Based on Material Decomposition, *Lect. Notes Comput*. Sc., 4142, pp. 624-635, 2006

Zhou, X., Hayashi, T., Hara, T., Fujita, H., Yokoyama, R., Kiryu, T., and Hoshi, H.: Automatic recognition of lung lobes and fissures from multi-slice CT images, *Proceedings of SPIE*, 5370, pp. 1629-1633, 2004.

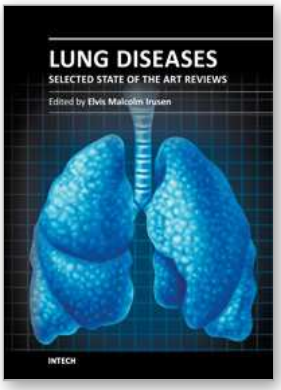

Lung Diseases - Selected State of the Art Reviews

Edited by Dr. Elvisegran Malcolm Irusen

ISBN 978-953-51-0180-2
Hard cover, 690 pages
Publisher InTech
Published online 02, March, 2012
Published in print edition March, 2012

The developments in molecular medicine are transforming respiratory medicine. Leading clinicians and scientists in the world have brought their knowledge and experience in their contributions to this book. Clinicians and researchers will learn about the most recent advances in a variety of lung diseases that will better enable them to understand respiratory disorders. This treatise presents state of the art essays on airways disease, neoplastic diseases, and pediatric respiratory conditions. Additionally, aspects of immune regulation, respiratory infections, acute lung injury/ARDS, pulmonary edema, functional evaluation in respiratory disorders, and a variety of other conditions are also discussed. The book will be invaluable to clinicians who keep up with the current concepts, improve their diagnostic skills, and understand potential new therapeutic applications in lung diseases, while scientists can contemplate a plethora of new research avenues for exploration.

How to reference

In order to correctly reference this scholarly work, feel free to copy and paste the following:

Kalicka Renata and Kuziemski Krzysztof (2012). Novel Methods for Diagnosis of Pulmonary Microangiopathy in Diabetes Mellitus, Lung Diseases - Selected State of the Art Reviews, Dr. Elvisegran Malcolm Irusen (Ed.), ISBN: 978-953-51-0180-2, InTech, Available from: http://www.intechopen.com/books/lung-diseases-selected-state-of-the-art-reviews/novel-methods-for-diagnosis-of-pulmonary-microangiopathy-in-diabetes-mellitus

INTECH
open science | open minds

InTech Europe
University Campus STeP Ri
Slavka Krautzeka 83/A
51000 Rijeka, Croatia
Phone: +385 (51) 770 447
Fax: +385 (51) 686 166
www.intechopen.com

InTech China
Unit 405, Office Block, Hotel Equatorial Shanghai
No.65, Yan An Road (West), Shanghai, 200040, China
中国上海市延安西路65号上海国际贵都大饭店办公楼405单元
Phone: +86-21-62489820
Fax: +86-21-62489821